

Transport Entropy of Vortex Motion in $\text{YBa}_2\text{Cu}_3\text{O}_7$

T. T. M. Palstra, B. Batlogg, L. F. Schneemeyer, and J. V. Waszczak
AT&T Bell Laboratories, 600 Mountain Avenue, Murray Hill, New Jersey 07974
 (Received 12 March 1990)

We report measurements of entropy transport due to vortex motion in single-crystal $\text{YBa}_2\text{Cu}_3\text{O}_7$. From these magnetothermal measurements we are able to determine thermodynamic properties, such as the transport line energy and superconducting phase boundary $T_c(H)$, as well as transport parameters associated with flux motion. Below T_c , the data are compared with the microscopic theory of Caroli and Maki. Interestingly, we also find large entropy transport in the fluctuation regime above T_c , which grows with applied field and for which no theory exists.

PACS numbers: 74.60.Ge, 74.30.Ek, 74.40.+k

In the high-temperature superconductors the vortex pinning energies can be of the order of thermal energies. This results, under the action of a driving force, in thermally activated flux motion and possibly to glassy or melting transitions. Such behavior has been intensely studied by measuring dissipative effects in, e.g., magneto-transport,^{1,2} magnetization,³ and mechanical experiments.^{4,5}

In this Letter we focus on an entirely different class of phenomena, the magnetothermal effects, by measuring the entropy or heat transport due to vortex motion. The thermally activated nature of vortex motion and, in particular, the absence of a critical current in a large part of the H - T phase diagram, make the layered cuprates ideally suited to study magnetothermal properties of superconductors. We will show that this gives new information about thermodynamic as well as transport properties. In addition, the transport entropy can be described in terms of excited states in the vortex core, which makes the connection to the microscopic theory.

An electrical current passed through the superconductor in the mixed state exerts a Lorentz force on the vortices. When the vortices move, they cause an electrical resistivity or dissipation. The vortex motion is accompanied by entropy (heat) flow, because a vortex has a different entropy than the unperturbed superconducting state. This heat flow (Ettinghausen effect) is in the direction of the Lorentz force, i.e., perpendicular to the electric and magnetic field, and can be expressed by⁶

$$U_\kappa = nTS_\phi v_\phi, \quad (1)$$

with n the areal density of vortices, T the temperature, S_ϕ the transport entropy per unit length vortex, and v_ϕ the average vortex velocity. The heat flow is compensated by regular heat conduction, $U_\kappa = \kappa dT/dy$ with κ the thermal conductivity, resulting in a temperature gradient across the sample. Combining this with the relation due to Josephson,⁷ $v_\phi = E/B$, we find that the transport line energy of a vortex is given by

$$U_\phi = TS_\phi = \kappa\phi_0 \frac{dT}{dy} \bigg/ \frac{dV}{dx}, \quad (2)$$

with dV/dx the voltage gradient in the direction of the electrical current. Therefore, three separate measurements are needed to calculate the vortex line energy: (1) the longitudinal voltage gradient due to an electrical current (i.e., electrical resistivity), (2) the transverse temperature gradient due to an electrical current, and (3) the thermal conductivity κ .

These measurements were performed on the same (microtwinning) single crystal of $\text{YBa}_2\text{Cu}_3\text{O}_7$ with dimensions $1.80 \times 0.71 \times 0.02$ mm³. The sample preparation (from a Cu-O flux) and extensive characterization have been reported elsewhere.⁸ The crystal was oxygenated for five weeks at 450°C to ensure oxygen homogeneity. Electrical contacts to the sample were made by evaporating silver on sputter-cleaned contact pads in a van der Pauw geometry. Vortex motion was induced by an ac electrical current of ~ 14 A/cm² at a frequency of 1 Hz. The magnetic field was generated by a 12-T superconducting solenoid. A differential Constantan-Chromel thermocouple was used to measure the transverse temperature gradient, resulting in thermal voltages < 40 nV, which were measured with a transformer-coupled lock-in amplifier. Simultaneously, the longitudinal electrical resistance was measured similarly. The temperature gradient was converted to a heat flow by measuring the thermal conductivity on the same sample, but with a different lead geometry, using a two-heater, one-thermometer technique.⁹ The thermometer was calibrated for each run against a calibrated carbon-glass thermometer. The heater output was chosen to be 50 μ W corresponding to a temperature difference of 150 mK between the heater contacts.

Figure 1 shows our main experimental results. In the upper panel (a) the magnetoresistance is shown in magnetic fields up to 12 T, or actually the longitudinal voltage gradient dV/dx for fixed current density $J \sim 14$ A/cm². The inset shows the zero-field resistive transition which is very sharp; the resistivity becomes zero at 87.5 K. At higher temperature $\rho(T)$ is linear with temperature and can be described by $\rho(T) = \rho_0 + \alpha T$ with a small intercept $\rho_0 = 5$ $\mu\Omega$ cm, and slope $\alpha = 0.456$ $\mu\Omega$ cm/K, indicative of very good crystal quality.

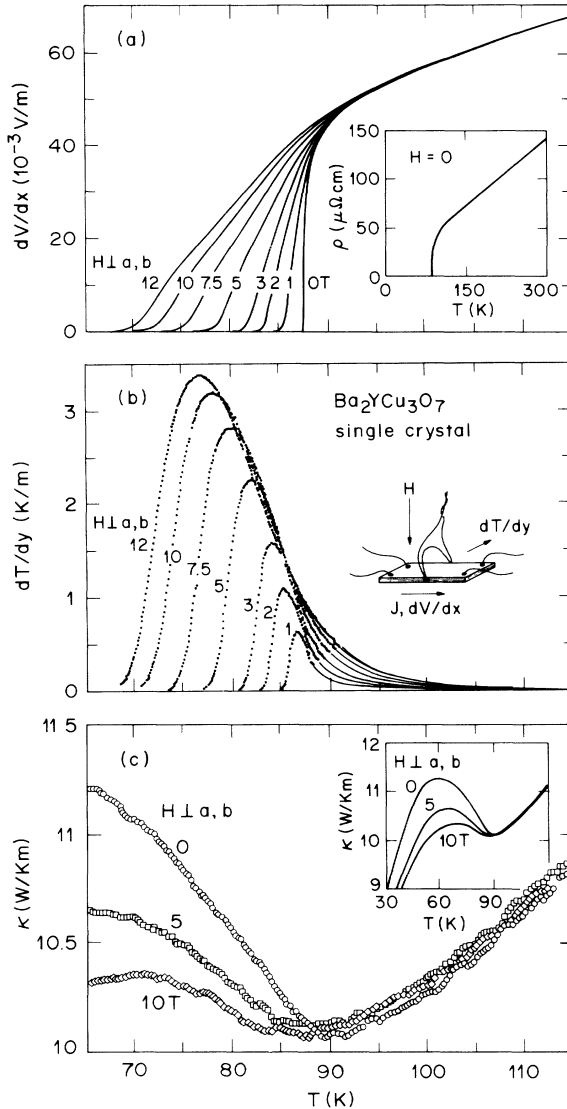


FIG. 1. (a) The longitudinal voltage gradient induced by an electrical current of 14 A/cm² in single-crystal YBa₂Cu₃O₇ for magnetic fields perpendicular to the basal plane from 0 to 12 T. Inset: The electrical resistivity in zero field up to 300 K. (b) The transverse temperature gradient induced by the same electrical current and magnetic fields. Inset: The actual lead configuration for the resistance and thermal-gradient measurements and the orientation of the magnetic field, which was always perpendicular to the Cu-O planes. Clearly, dT/dy is already nonzero far above T_c , attaining a maximum of the order of ~ 1 K/m around T_c , and approaching zero again at lower temperature. (c) The thermal conductivity for three magnetic fields: 0, 5, and 10 T. Inset: Data on an expanded temperature scale.

The middle panel (b) shows the transverse temperature gradient dT/dy as a function of temperature for fixed magnetic fields up to 12 T at the fixed current density $J \sim 14$ A/cm². The inset shows the actual lead configuration for the resistance and thermal-gradient measurements and the orientation of the magnetic field, which was always perpendicular to the Cu-O planes. Clearly, dT/dy is already nonzero far above T_c , attaining a maximum of the order of ~ 1 K/m around T_c , and approaching zero again at lower temperature.

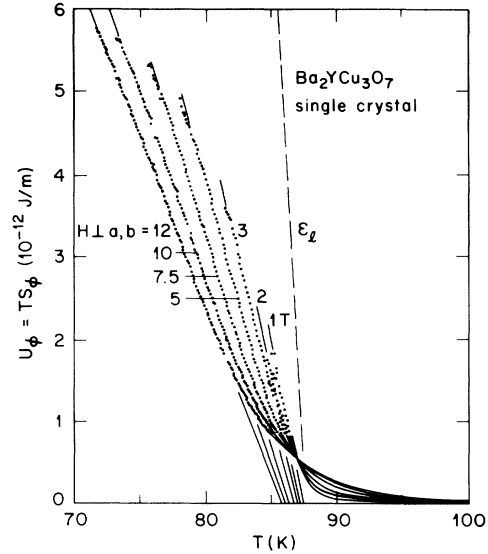


FIG. 2. Temperature dependence of the transport line energy U_ϕ for magnetic fields perpendicular to the basal plane between 1 and 12 T for single-crystal YBa₂Cu₃O₇. Also shown is the free line energy ϵ_l .

In the lower panel (c) the thermal conductivity $\kappa(T)$ is given as a function of temperature for magnetic fields of 0, 5, and 10 T. Above T_c the thermal conductivity κ decreases with decreasing temperature, but starts to increase near T_c and goes through a broad maximum at around 60 K. This broad peak is effectively reduced by applying a magnetic field. The data are shown in the inset on a larger temperature scale. It should be noticed that between 65 and 115 K the changes of κ are only $\sim 10\%$, and therefore contribute only a little to the temperature dependence of the transport line energy U_ϕ . Knowing $\kappa(T, H)$ is necessary to convert the temperature gradient into an energy flow and to calculate the absolute magnitude of U_ϕ . The magnitude of $\kappa \approx 10$ W/mK compares well with other single-crystal data,¹⁰ but is approximately a factor of 3 larger than polycrystalline data.¹¹

Combining these measurements allows us to calculate the transport line energy $U_\phi(T, H)$. This parameter is shown in Fig. 2 as function of temperature between 70 and 110 K for magnetic fields between 1 and 12 T.

Before discussing the present results we outline the physical significance of the transport entropy. The transport entropy is the entropy of the bound core states of the vortices, i.e., states in the vortex core with energies smaller than the gap energy.^{12,13} In the absence of excitations, at $T=0$, vortex motion does not involve entropy transport. Also, the extended states, with excitation energies larger than the energy gap, do not contribute to the transport entropy at finite temperature. Therefore, the transport line energy is smaller than the free line energy. Furthermore, because of the general suppression of the order parameter near T_c and the overlap of the

vortices, the transport entropy should go to zero at T_c . The calorimetric entropy, in contrast, goes to the normal-state value at T_c . As thermodynamics requires that S_0 also goes to zero, at $T=0$, S_0 has a maximum between $T=0$ and T_c .

Using a time-dependent Ginzburg-Landau formalism, Caroli and Maki¹⁴ found general expressions for the transport entropy near H_{c2} :

$$U_0 = TS_0 = \phi_0 \langle M \rangle L(t), \quad (3)$$

with $\langle M \rangle$ the equilibrium magnetization, and $L(t)$ a transport coefficient. $L(t)$ was found to vary smoothly between 1 and 2 in the dirty limit, and is of the order of l/ξ in the pure limit, with l the mean free path. This relates the thermodynamic aspect of U_0 to the equilibrium magnetization, and the transport aspect is captured in the transport coefficient $L(t)$.

This is in qualitative agreement with the very few studies on low- T_c materials.¹⁵⁻¹⁷ In particular, the vanishing of S_0 at H_{c2} has been observed experimentally. However, magnetothermal measurements are difficult to perform in conventional superconductors because pinning leads to nonlinear I - V response, and (large) depinning currents are incompatible with the adiabatic conditions needed to measure the magnetothermal effects. In contrast, the thermally activated nature of flux motion in high- T_c superconductors yields linear response over a wide range of driving forces. This makes these materials ideally suited to study magnetothermal effects in much greater detail than is possible with conventional superconductors.

Our results on $\text{YBa}_2\text{Cu}_3\text{O}_7$ are best discussed in three temperature ranges: the behavior of U_0 at T_c , below T_c , and above T_c . Experimentally, we find that the transport line energy depends linearly on temperature from the lowest accessible temperature to close to $T_c(0)$. This emphasizes the theoretical relation of U_0 with $\langle M \rangle$, which also goes linearly to zero at T_c . We obtain $T_c(H)$ by extrapolating the linear part of U_0 to zero. This estimate of $T_c(H)$ is shown in Fig. 3. The resulting upper critical fields depend linearly on temperature with a slope $-dH_{c2}/dT = 7 \pm 1$ T/K. Only for the lowest fields (1 and 2 T), where the experimental resolution is the poorest, are there deviations from this line. This upper-critical-field slope extrapolates to an upper critical field of $H_{c2}^{a,b}(0) \approx 400$ T, and corresponds to a coherence length of about $\xi_{a,b}(0) \approx 9$ Å.

Alternatively, we can use a more conventional way to define T_c , by calculating the transport specific heat, i.e., the specific heat of the bound states of the vortex core, using $c_p = -T \partial S_0 / \partial T$. In the inset of Fig. 3 we have shown an example of c_p for a magnetic field of 10 T. [Note that 1 mole contains 5×10^{11} m flux line at 10 T and thus $\Delta c_p / T(T_c) \approx 3$ mJ/moleK² at 10 T.] Using the conventional "midpoint definition" of T_c , we consistently find a lower value for $T_c(H)$ than if determined directly from U_0 , for all magnetic fields. This results

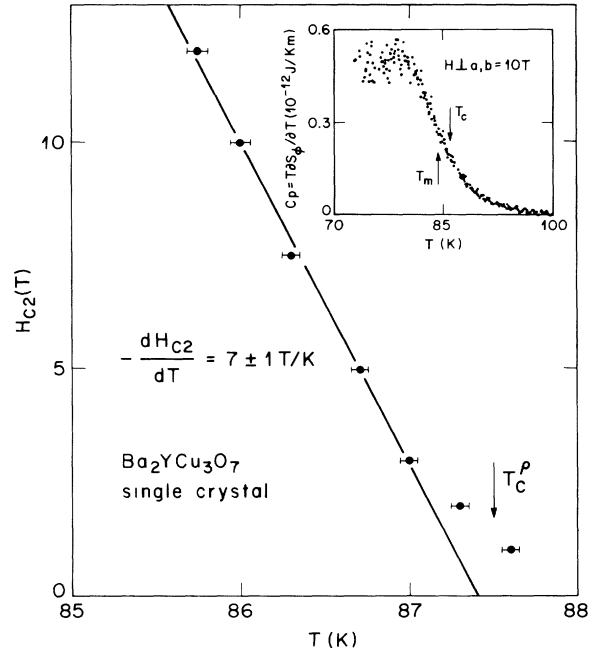


FIG. 3. Temperature dependence of the upper critical field H_{c2} for single-crystal $\text{YBa}_2\text{Cu}_3\text{O}_7$. Inset: The vortex transport specific-heat anomaly near T_c in a magnetic field of 10 T (see text).

also in a lower value for the upper-critical-field slope, $-dH_{c2}/dT \approx 3.5$ T/K. This illustrates the sensitivity of a criterion in the present specific-heat jump to define $T_c(H)$. We think that the $T_c(H)$ determination using the $U_0(T)$ data directly is less ambiguous and represents the thermodynamic value.

This value of $-dH_{c2}/dT = 7 \pm 1$ T/K can be compared with calorimetric specific-heat measurements and equilibrium magnetization measurements. Specific-heat measurements, using a midpoint definition, resulted in a value of $-dH_{c2}/dT$ ranging from 3 (Ref. 18) to 6 T/K.¹⁹ Magnetization measurements obtained a value of 2 T/K.²⁰ The discrepancy with some specific-heat results can be understood by the reason given above. The discrepancy with the magnetization measurements is more noteworthy, because of the intimate relation of these two quantities [Eq. (3)].

Now we turn to the properties below T_c . We can compare the transport line energy U_0 with the vortex free line energy ϵ_l , given by

$$\epsilon_l(T) \approx \frac{\mu_0 \phi_0^2}{4\pi\lambda^2} \ln \kappa_{\text{GL}}. \quad (4)$$

Various experimental techniques find consistently for the magnetic penetration depth in the basal plane $\lambda_{a,b} \approx 1400$ Å.²¹⁻²³ This results in a zero-temperature free line energy $\epsilon_l(0) = 6.9 \times 10^{-11}$ J/m. Using the two-fluid-model temperature dependence of λ , we find near T_c a slope of $d\epsilon_l/dT = 3.2 \times 10^{-12}$ J/Km, as shown in Fig. 2. Comparing ϵ_l with U_0 , we have to take the low-field limit of U_0 for which the overlap of the vortices is

small. Extrapolating the linear field dependence of dU_ϕ/dT to zero field, we find a slope for the transport line energy of $dU_\phi/dT = 7.6 \times 10^{-13}$ J/Km. Thus, in this temperature range the energy transported by a vortex is about 25% of the vortex free energy.

The third part of the data we discuss is the behavior of U_ϕ above T_c . From Fig. 2 it is clear that we observe above T_c a pronounced entropy transport contribution. Apparently, the incipient formation of vortices above T_c is a sufficient condition for entropy transport. Interestingly, U_ϕ increases linearly with magnetic field, which is in marked contrast to the concept that a magnetic field suppresses superconducting fluctuations. It should be kept in mind that analysis of this regime is complicated, because both the normal and the superfluid components contribute to dissipation.

Through the Onsager relations we can relate the Ettinghausen effect to other thermomagnetic effects. Namely, vortices are not only driven by electrical currents, but also by a temperature gradient.^{24,25} The physical origin is that at higher temperatures the vortex density is higher (smaller magnetization), but the larger magnetic penetration depth repels the vortices more strongly. As a result the vortices are driven to lower temperature. We can express the thermal force as $f_{th} \approx (\partial U_\phi / \partial T) \nabla T$. Using our experimental values near T_c and, e.g., $\nabla T = 10^2$ K/m, we find that $f_{th} \approx 6 \times 10^{-11}$ N/m. This is equivalent to the Lorentz force $f_L = J\phi_0$ due to a current density $J \approx 3 \times 10^4$ A/m². Thus, a temperature gradient acts like a Lorentz force on vortices.

Using our experimental results we can evaluate other thermomagnetic effects. The Nernst effect should be readily observable. Namely, an applied temperature gradient $\nabla T \sim 10^2$ K/m will induce a transverse voltage of the order of 10^{-3} V/m. Also other measurements will be affected, e.g., the Hall effect. A Hall-effect measurement will probe in addition to the carrier concentration the thermopower of the temperature gradient induced by vortex motion. This might explain the anomalous behavior of the Hall angle below T_c .²⁶ Likewise, a thermal-conductivity measurement in a magnetic field probes, besides the electron and phonon conduction, a heat flow $nv_\phi U_\phi$ due to vortex motion. This contributes in our experiments only 0.1% of the imposed heat current, which is just beyond our experimental resolution. In systems with a higher vortex mobility this might be a pronounced effect.

In conclusion, we have measured the transport entropy of vortices in single-crystal YBa₂Cu₃O₇. Below T_c the transport line energy is a factor of 4 smaller than the free line energy. Above T_c the transport entropy exhibits a pronounced fluctuation effect, which is not understood. From these measurements we found an upper-critical-field slope of $-dH_{c2}/dT = 7$ T/K, corresponding to an in-plane coherence length $\xi_{a,b} \approx 9$ Å. Our thermomagnetic effects are shown to be large in YBa₂Cu₃O₇ and can be evaluated readily from these measurements.

We gratefully acknowledge stimulating discussions with S. N. Coppersmith, A. T. Fiory, F. Gygi, A. F. Hebard, H. F. Hess, D. A. Huse, and M. Inui. The collaboration of J. E. Graebner in the present measurements is especially acknowledged.

¹T. T. M. Palstra, B. Batlogg, L. F. Schneemeyer, and J. V. Waszczak, Phys. Rev. Lett. **61**, 1662 (1988); Appl. Phys. Lett. **54**, 764 (1989); Phys. Rev. B **41**, 6621 (1990), and references therein.

²R. H. Koch, V. Foglietti, W. J. Gallagher, G. Koren, A. Gupta, and M. P. A. Fisher, Phys. Rev. Lett. **63**, 1511 (1989).

³A. P. Malozemoff, in *Physical Properties of High Temperature Superconductors*, edited by D. M. Ginsberg (World Scientific, Singapore, 1989).

⁴P. L. Gammel, L. F. Schneemeyer, J. V. Waszczak, and D. J. Bishop, Phys. Rev. Lett. **61**, 1666 (1988).

⁵A. Gupta, P. Esquinazi, and H. F. Braun, Phys. Rev. B **39**, 12271 (1989).

⁶R. P. Huebener, in *Magnetic Flux Structures in Superconductors*, edited by R. P. Huebener, Springer Series in Solid State Sciences Vol. 6 (Springer-Verlag, Berlin, 1979), Secs. 7.6 and 9.3.

⁷B. D. Josephson, Phys. Lett. **16**, 242 (1966).

⁸L. F. Schneemeyer, J. V. Waszczak, T. Siegrist, R. B. van Dover, L. W. Rupp, B. Batlogg, R. J. Cava, and D. W. Murphy, Nature (London) **328**, 601 (1987).

⁹The thermometer and heaters were fabricated by J. E. Graebner and described in J. E. Graebner, Rev. Sci. Instrum. **60**, 1123 (1989).

¹⁰S. J. Hagen, Z. Z. Wang, and N. P. Ong (to be published).

¹¹C. H. Uher and A. B. Kaiser, Phys. Rev. B **36**, 5680 (1987).

¹²C. Caroli, P. G. de Gennes, and J. Matricon, Phys. Lett. **9**, 307 (1964).

¹³A. L. Fetter and P. C. Hohenberg, in *Superconductivity*, edited by R. D. Parks (Marcel Dekker, New York, 1969), Vol. 2.

¹⁴C. Caroli and K. Maki, Phys. Rev. **164**, 591 (1967); K. Maki, Physica (Utrecht) **55**, 124 (1971).

¹⁵P. R. Solomon and F. A. Otter, Phys. Rev. **164**, 608 (1967).

¹⁶R. P. Huebener and A. Seher, Phys. Rev. **181**, 701 (1969).

¹⁷F. Vidal, Phys. Rev. B **8**, 1982 (1973).

¹⁸S. Inderhees, M. B. Salomon, N. Goldenfeld, J. P. Rice, B. G. Pazol, D. M. Ginsberg, J. Z. Liu, and G. W. Crabtree, Phys. Rev. Lett. **60**, 1178 (1988); (private communication).

¹⁹J. E. Graebner (unpublished).

²⁰U. Welp, W. K. Kwok, G. W. Crabtree, K. G. Vandervoort, and J. Z. Liu, Phys. Rev. Lett. **62**, 1908 (1989).

²¹A. T. Fiory, A. F. Hebard, P. M. Mankiewich, and R. E. Howard, Phys. Rev. Lett. **61**, 1419 (1988).

²²D. R. Harshman, L. F. Schneemeyer, J. V. Waszczak, G. Aeppli, R. J. Cava, B. Batlogg, L. W. Rupp, E. J. Ansaldo, and D. L. Williams, Phys. Rev. B **39**, 851 (1989).

²³L. Krusin-Elbaum, R. L. Greene, F. Holtzberg, A. P. Malozemoff, and Y. Yeshurun, Phys. Rev. Lett. **62**, 217 (1989).

²⁴M. J. Stephen, Phys. Rev. Lett. **16**, 801 (1966).

²⁵A. G. van Vijfeijken, Phys. Lett. **23**, 65 (1966).

²⁶Y. Iye, S. Nakamura, and T. Tamegai, Physica (Amsterdam) **159C**, 616 (1989).